

Spin relaxation in SiGe two-dimensional electron gases

Charles Tahan and Robert Joynt
Physics Department, University of Wisconsin-Madison
(Dated: January 2004)

Silicon is a leading candidate material for spin-based devices, and two-dimensional electron gases (2DEGs) formed in silicon heterostructures have been proposed for both spin transport and quantum dot quantum computing applications. The key parameter for these applications is the spin relaxation time. Here we apply the theory of D'yakonov and Perel' (DP) to calculate the electron spin resonance linewidth of a silicon 2DEG due to structural inversion asymmetry for arbitrary static magnetic field direction at low temperatures. We estimate the Rashba spin-orbit coupling coefficient in silicon quantum wells and find the T_1 and T_2 times of the spins from this mechanism as a function of momentum scattering time, magnetic field, and device-specific parameters. We obtain agreement with existing data for the angular dependence of the relaxation times and show that the magnitudes are consistent with the DP mechanism. We suggest how to increase the relaxation times by appropriate device design.

Introduction Electron spins in silicon have been proposed as an attractive architecture for spintronics and quantum information devices. The inherently low and tunable spin-orbit coupling (SOC) in silicon heterostructures and the possibility of eliminating hyperfine couplings by isotopic purification bodes well for quantum coherent spin-based qubits and spin transport. Early experiments together with theory have shown that coherence times can be upwards of three orders of magnitude longer than in GaAs.[1, 2, 3, 4]

Energy relaxation of localized spin states has attracted theoretical attention [5, 6, 7, 8, 9] and experimental effort [3, 10] for decades, and this activity has recently revived in the context of quantum computation. The idea is to store quantum information in the spin of a single electron confined in a semiconductor structure, either attached to a donor atom or confined electrostatically in a quantum dot. Spin transport, also of great interest, encodes information in the spin states of an ensemble of electrons. In both cases, electron spin resonance (ESR) measurements of spin relaxation provide a key and available measure of spin coherence properties of electrons in silicon quantum wells, though not a one-to-one correspondence. Our aim in this paper is to explain some existing ESR results for silicon 2DEGs at low temperatures and to make predictions for future experiments.

The structures that concern us here are layered semiconductor devices of Si and SiGe. The active layer is the quantum well (QW) that confines the electrons in the growth direction. This layer will be assumed to be composed of pure, strained silicon. We shall also neglect any roughness at the the Si/SiGe interfaces. Devices made in this way are commonly referred to in the semiconductor industry as MODFETs and are designed to maximize mobility. Figure 1 introduces two example structures.

Extensive theoretical work has been done on spin relaxation in GaAs and other III-V materials. The developments that began with the theory of D'yakonov and Perel' [11, 12, 13] are most relevant for our purposes. These authors found that fluctuating effective magnetic fields due to momentum scattering in the presence of

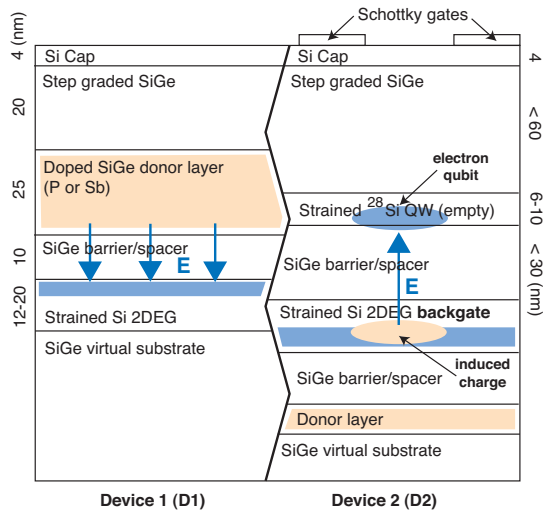


Figure 1: Strong, internal electric fields are common in silicon quantum well devices. *D1*: A typical, high-mobility SiGe heterostructure uses a donor layer to populate a high-density 2DEG. The charge separation results in an $E_z \sim 10^6$ V/m. *D2*: A proposed quantum dot quantum computer [14] which utilizes a tunnel-coupled backgate to populate the quantum well without the need for a nearby donor layer. Here, $E_z > 10^5$ V/m due to the image potential formed on the backgate.

SOC is the dominant spin relaxation mechanism in semiconductor 2DEGs for low temperatures. Here, we start with this assumption and use a general spin-density matrix approach to calculate the relaxation times of a 2DEG in the presence of a static magnetic field, including explicitly the angular dependence.

In the next section we discuss the origin and magnitude of the SOC in realistic heterostructures. The section following that presents our calculation. Lastly, we compare with experiment and discuss the implications for device design.

Spin-orbit coupling The strong macroscopic electric

fields inside heterostructure QWs are important for understanding SOC, especially in silicon. These fields are also device-specific, so we carry out our calculations on the two representative structures in Figure 1. Both devices have square QWs, with equal barriers on the top and bottom interface. The first is typical of MODFETs and employs a donor layer above the QW in order to populate it. This charge separation produces an electric field between the two layers (across the barrier or spacer layer) which can be approximated by

$$E^{D1} \approx \frac{en_s}{\epsilon_0 \epsilon_{Si}} = -6 \times 10^6 \text{ V/m}, \quad (1)$$

where $n_s = 4 \times 10^{15} \text{ m}^{-2}$ is the density of electrons in the 2DEG for Device 1, e is the charge of an electron, and ϵ_i are the dielectric constants. We assume that *the QW is populated only by donor-layer electrons*, leaving an equal amount of positive charge behind. The second structure is one that has been proposed for use in a quantum computer device.[14] It utilizes a near-lying, tunnel-coupled backgate 2DEG ($< 30 \text{ nm}$ away) together with Schottky top-gates to populate the QW selectively. This situation also results in a strong electric field due to the image potential on the back gate. For one qubit, this can be estimated as

$$E^{D2} \approx \frac{e}{4\pi\epsilon_0\epsilon_{Si}d^2} = 3 \times 10^5 \text{ V/m}, \quad (2)$$

where $d = 20 \text{ nm}$ is the distance from the QW to the back gate for Device 2. Schottky top-gates and other device parameters can augment or reduce this growth-direction electric field nominally up to the breakdown field of silicon, $3 \times 10^7 \text{ V/m}$.[15] Indeed, this field can actually be smaller than that due to the top-gates in certain dot configurations.

The shift of the electron g-factor from its free-electron value $g_0 = 2.00232$ is one measure of SOC in a system. It is quite small in bulk silicon and depends on the magnetic field direction in the (elliptical) conduction band minima ($\Delta g_{\parallel} \approx -0.003$, $\Delta g_{\perp} \approx -0.004$).[10] However, it is difficult to reliably extract the SOC strength in a 2DEG from Δg . Many parameters (e.g., strain, barrier penetration, Ge content ($g_{Ge} = 1.4$), non-parabolicity of the band minima) influence the magnitude and sign of Δg and it may show considerable sample dependence. The non-parabolicity effects are especially sensitive to the electron density within the QW and can hide the magnitude of SOC within a system.[16]

In these silicon heterostructures, SOC is dominated by inversion asymmetry within the device. The spin-orbit (SO) Hamiltonian to first order in momentum is given in an arbitrary electrostatic potential V by

$$H_{SO} = \frac{\hbar \nabla V \cdot (\vec{\sigma} \times \mathbf{p})}{4m^2c^2},$$

where σ_i are the Pauli matrices. In Si heterostructures, the macroscopic fields, which do not average out, are more important than the atomic electric fields. In the

noncentrosymmetric III-V materials such as GaAs, this is not necessarily the case and the resulting Dresselhaus or *bulk* inversion asymmetry fields are usually dominant. The asymmetry considered here, due either to an interface, charge distribution, or external potential, is usually called Rashba or *structural* inversion asymmetry.

The Rashba term comes directly from the SO Hamiltonian if we assume one, dominant symmetry-breaking electric field in the structure and average over a momentum state. In a QW, as we have pointed out above, the electric field is in the growth (z) direction and thus the z -component of the above dot-product is selected and we obtain

$$H_R^{2D} = \alpha(p_x\sigma_y - p_y\sigma_x) \propto E_z(\vec{\sigma} \times \mathbf{p})_z, \quad (3)$$

which is then the Rashba-Bychkov Hamiltonian.[17]

Strictly speaking, as de Andrade e Silva *et. al.* point out [18], the conduction-band-edge profile, E_c , and the space charge separation (or applied electrostatic field), E_z , contribute separately and sometimes dissimilarly to the SOC. For example, the wavefunction discontinuity (band offset) across a material-interface can cause Rashba spin-splitting itself. However, in devices of the type considered here, the macroscopic field should be the main contribution. These same authors have derived an expression for α in the Kane model for GaAs. We have adapted their work for Si, using a 5-parameter 8-band Kane model. This is 8 bands including spin, which means just the lowest conduction band and the three highest valence bands. We find

$$\alpha = \frac{\sqrt{2}PP_z\Delta_d}{\hbar(E_{v1} + \Delta_d)^2E_{v2}}eE_z. \quad (4)$$

Here $P = \hbar\langle X|p_x|S\rangle/im$, $P_z = \hbar\langle Z|p_z|S\rangle/im$, $\Delta_d = 0.044 \text{ eV}$ is the spin-orbit splitting of the two highest conduction bands, $E_{v1} = 3.1 \text{ eV}$ is the direct gap of the strained sample, and $E_{v2} = 7 \text{ eV}$ is the gap between the conduction band minimum and the lowest of the three valence bands. (These are the 5 parameters mentioned above.) m is the bare electron mass. The matrix elements that define P and P_z are to be taken between the cell-periodic functions of the indicated symmetry at the position of the conduction-band minimum. Unfortunately, these are not well known in Si, since other bands contribute. If we use the naive relations between these parameters and the effective mass: $2mP^2/\hbar^2E_{v1} = m/m_{\perp} - 1$ and $2mP_z^2/\hbar^2E_{v2} = m/m_{\parallel} - 1$, with m_{\perp} and m_{\parallel} being the transverse and longitudinal effective masses at the conduction band minimum, we find

$$\alpha \approx 2.5 \times 10^{-7} E \text{ m/s} \quad (5)$$

if E is given in V/m. This value can easily change by a factor of 2-4 with small changes in the input parameters (usually increasing).

Wilamowsky *et. al.* [19], using conduction electron spin resonance (CESR), have measured $\alpha \approx 5.94 \text{ m/s}$ ($\alpha e/\hbar = 0.55/\sqrt{2} \times 10^{-12} \text{ eV}\cdot\text{cm}$ in their units) [25] in

Parameter	Value	Barrier Ge, $x = 0.25$
Δ	0.044 eV	
E_g (indirect)	$1.11 - 0.4x$ eV	1.01 eV
E_g (direct)	$-12 \epsilon_{ } + 3.3$ eV	3.175 eV
$m_{\perp}^*/m_{ }^*$	$0.19m_0/0.98m_0$	
ϵ_{Si}	11.8	
$\epsilon_{ }(x)$	$(a_{ }(x) - a_{Si})/a_{Si}$	0.01 Å
$a_{ }(x)$	$(1-x)a_{Si} + xa_{Ge}$	5.48 Å
a_{Si}/a_{Ge}	5.431 Å/5.657 Å	

Table I: Physical values for a strained silicon layer used for calculations within this paper. The layer is fully relaxed to a $\text{Si}_{1-x}\text{Ge}_x$ layer so that the in-plane lattice constant is $a_{||}(x)$.

a $\text{Si}_{0.75}\text{Ge}_{0.25}/\text{Si}/\text{Si}_{0.75}\text{Ge}_{0.25}$ QW where the strained-silicon layer was roughly 12–20 nm. Carrier concentrations were $n_s \approx 4 \times 10^{15} \text{ m}^{-2}$. These numbers correspond to our Device 1 parameters. Our equations then give

$$\alpha^{D1} \approx 1.6 \text{ m/s for } E_z = 6.1 \times 10^6 \text{ V/m.}$$

Theory compares in order of magnitude and we believe that our estimation has some utility as a guide for device design, though it is clear that a more comprehensive theory for α in silicon is needed.

For Device 2, $\alpha^{D2} \approx 0.076 \text{ m/s}$ for $E_z = 3 \times 10^5 \text{ V/m}$. This device remains to be built. For Device 1, we can also predict the zero magnetic field spin-splitting in a silicon 2DEG using $|\epsilon_+ - \epsilon_-| \leq 2\alpha p_F$,

$$2\alpha p_F = 2\alpha \hbar \sqrt{\frac{4\pi n_s}{4}} \approx 0.23 \mu\text{eV},$$

where 4 is the degeneracy factor in silicon (spin+valley). This has not yet been directly measured to our knowledge. Taking a Zeeman splitting of $g\mu_B B = 0.23 \mu\text{eV}$ with a g-factor of 2, this implies an internal, in-plane, effective magnetic field—the so-called *Rashba field*—of roughly 19 Gauss, which is the direct result of SOC in the silicon 2DEG of Device 1.

Spin relaxation We wish to consider the combined effects of the SO Hamiltonian

$$H_R^{2D} = \alpha(p_x \sigma_y - p_y \sigma_x)$$

and the scattering Hamiltonian. The scattering may be from phonons or from static disorder. We take the semiclassical approach, in which the effect of scattering is to cause transitions at random intervals from one wavepacket centered at \vec{p} with $\epsilon_{\vec{p}} = \epsilon_F$ to another centered at \vec{p}' with $\epsilon_{\vec{p}'} = \epsilon_F$, where ϵ_F is the Fermi energy. This corresponds to a random switching in the direction of the effective magnetic field that acts on the spin degree of freedom. This is the D'yakonov-Perel' mechanism of spin relaxation.[11, 12] The measured quantity in the continuous-wave experiments carried out on 2DEGs is

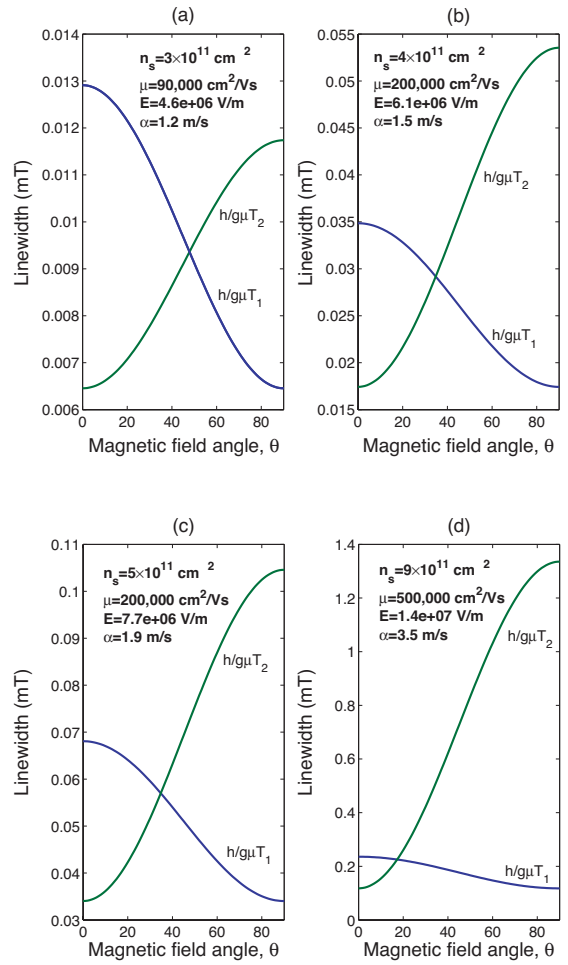


Figure 2: ESR linewidths in Gauss as a function of static magnetic field direction (where $\theta = 0$ is perpendicular to the 2DEG plane) for specific values of 2DEG density and Rashba asymmetry. The quantum well is assumed to be completely donor-layer populated and as such, α is calculated directly with Eq. 5 as a function of the 2DEG density.

T_2 , the transverse relaxation time, while pulsed experiments can also measure T_1 , the longitudinal relaxation time. For our purposes, a density matrix approach is the natural one, since we will eventually want to perform an ensemble average over all possible scattering sequences. Since the physical model of spins in a random time-dependent magnetic field is the same as that for relaxation of nuclear spins in liquids, the Redfield technique may be used.[20]

The 2×2 density matrix ρ allows us to compute the expectation values of the spin by

$$\langle \sigma_i \rangle = \text{Tr} \{ \sigma_i \rho \}.$$

For a single electron described by the Hamiltonian H , we have the equation of motion

$$\frac{d\rho}{dt} = \frac{i}{\hbar} [\rho, H].$$

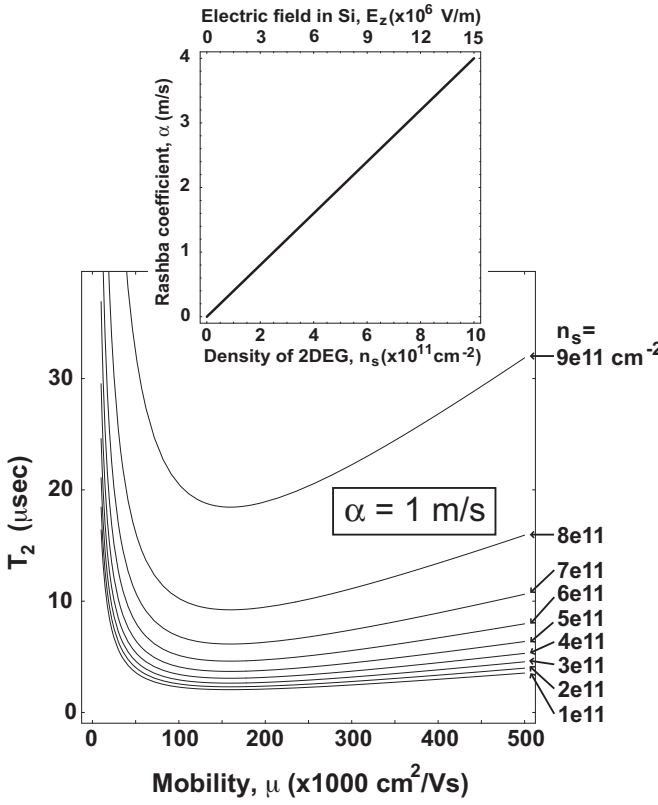


Figure 3: ESR linewidth lifetime T_2 from Eq. 8 for constant asymmetry coefficient, $\alpha = 1$ m/s, as a function of 2DEG mobility, μ , and density, n_s . For donor-layer populated quantum wells, divide the times listed by α^2 : $T_2(\alpha) = T_2(\alpha = 1)/\alpha^2$. The magnetic field is assumed to be $B = 0.33$ Tesla, perpendicular to the plane of the 2DEG. Inset: Rashba asymmetry coefficient α from Eq. 5 as a function of 2DEG density, assuming all the charges in the 2DEG come from the donor layer.

For our case, the spin Hamiltonian is

$$H = -g^* \mu_B \mathbf{B}_{ext} \hat{n} \cdot \vec{\sigma} / 2 + H_1(t), \quad (6)$$

where \hat{n} is the direction of the steady external field \mathbf{B}_{ext} and

$$H_1(t) = \sum_{i=x,y} h^i(t) \sigma_i.$$

The statistics of this random field are determined by $\chi^i(t - t') = \overline{h^i(t)h^i(t')}$ and $\overline{h^i(t)h^j(t')} = 0$ for $i \neq j$. We also define

$$\chi^i(\omega) = \int_{-\infty}^{\infty} d\tau e^{i\omega\tau} \overline{h^i(0)h^i(\tau)}.$$

We then find

$$1/T_1 = 2 [\chi^{t1}(\omega_L) + \chi^{t2}(\omega_L)] / \hbar^2,$$

and

$$1/T_2 = [\chi^{t1}(\omega_L) + \chi^{t2}(\omega_L) + 2\chi^\ell(0)] / \hbar^2.$$

where $\omega_L = eB/m$ is the Larmor frequency, $t1$ and $t2$ are two axes perpendicular to \hat{n} , and ℓ lies along \hat{n} . In particular, let \vec{B}_{ext} point along the direction $B_x \hat{x} + B_z \hat{z} = \sin \theta \hat{x} + \cos \theta \hat{z}$, where θ is the angle to the normal of the plane of the 2DEG. Then the longitudinal fluctuations χ^ℓ , which are quadratic in the field, are proportional to $\sin^2 \theta$ and the transverse ones $\chi^{t1,t2}$ to $\cos^2 \theta$. Thus

$$1/T_1(\theta) = 2 [\cos^2 \theta \chi^x(\omega_L) + \chi^y(\omega_L)] / \hbar^2 \quad (7)$$

while

$$1/T_2(\theta) = [\cos^2 \theta \chi^x(\omega_L) + \chi^y(\omega_L) + 2 \sin^2 \theta \chi^x(0)] / \hbar^2. \quad (8)$$

Scattering events follow Poisson statistics, and for a circular Fermi surface the random field is constant in magnitude, so we find

$$\overline{h^i(0)h^i(\tau)} = \langle h_x^2 \rangle e^{-t/\tau} = \frac{1}{2} \alpha^2 p_F^2 e^{-t/\tau_p},$$

and

$$\begin{aligned} \chi^x(\omega) = \chi^y(\omega) &= \frac{1}{2} \alpha^2 p_F^2 \operatorname{Re} \int_{-\infty}^{\infty} dt e^{i\omega t - |t|/\tau_p} \\ &= \alpha^2 p_F^2 \operatorname{Re} \frac{1}{i\omega - 1/\tau_p} \\ &= \frac{\alpha^2 p_F^2 \tau_p}{1 + \omega^2 \tau_p^2}. \end{aligned}$$

τ_p is the momentum relaxation time. Note that these formulas assume s-wave scattering.

The zero-frequency limit of these formulas agrees with the recent results of Burkov and MacDonald [21] [see their Eq.(17)]. They do not agree with the formulas in Wilamowski *et. al.* [19], [see, e.g., their Eq.(3)] who state that the relaxation from the DP mechanism should vanish when $\theta = 0$. This is not consistent with our results.

The DP mechanism has the nice feature that it is relatively easy to isolate experimentally. It is strongly anisotropic in the direction of the applied field compared to other mechanisms. To illustrate this we plot the ESR linewidths as a function of field angle in Fig. 2. What is most striking is the opposite dependence on angle for the rates $1/T_1$ and $1/T_2$, with $1/T_2$ maximized when the field is in the plane of the 2DEG, while $1/T_1$ is maximized when the field is perpendicular to the plane of the 2DEG. Physically, this comes from the fact that the electric field is perpendicular, so that the fluctuations of the effective magnetic field are in the plane. Longitudinal relaxation (T_1) is due to fluctuations perpendicular to the steady field, while transverse relaxation (T_2) is due to fluctuations both perpendicular and parallel to the steady field. This mechanism has the characteristic that the change in $1/T_1$ as the field is rotated through 90 degrees is always a factor of two. The change in $1/T_2$ is frequency- and lifetime-dependent, with the anisotropy increasing as the mobility increases.

Source	Linewidth	Anisotropy
Ref. [2] $\mu \sim 90 \times 10^3 \text{ cm}^2/\text{V}\cdot\text{s}$ $n_s \sim 3 \times 10^{15} \text{ m}^{-2}$ Pulsed-ESR light populated	Exp.: $T_2^{B\parallel z} = 3 \mu\text{s}$ $T_2^{B\perp z} = 0.24 \mu\text{s}$ $T_1^{B\parallel z} = 2 \mu\text{s}$ $T_1^{B\perp z} = 3 \mu\text{s}$ Pred.: $T_2^{B\parallel z} = 5.3 \mu\text{s}$ $T_2^{B\perp z} = 2.9 \mu\text{s}$ $T_1^{B\parallel z} = 2.65 \mu\text{s}$ $T_1^{B\perp z} = 5.3 \mu\text{s}$	$T_2^{B\parallel z}/T_2^{B\perp z} = 12.5$ $T_1^{B\parallel z}/T_1^{B\perp z} = 0.67$ $T_2^{B\parallel z}/T_2^{B\perp z} = 1.8$ $T_1^{B\parallel z}/T_1^{B\perp z} = 0.5$
Ref. [19] $\mu \sim 200 \times 10^3 \text{ cm}^2/\text{V}\cdot\text{s}$ $n_s \sim 4 \times 10^{15} \text{ m}^{-2}$ CW-ESR (10 K) donor populated	Exp.: $T_2^{B\parallel z} = 2.3 \mu\text{s}$ $T_2^{B\perp z} = 0.75 \mu\text{s}$ Pred.: $T_2^{B\parallel z} = 2 \mu\text{s}$ $T_2^{B\perp z} = 0.64 \mu\text{s}$	$T_2^{B\parallel z}/T_2^{B\perp z} = 3.1$ $T_2^{B\parallel z}/T_2^{B\perp z} = 3.1$ $T_1^{B\parallel z}/T_1^{B\perp z} = 0.5$
Ref. [1] $\mu \sim 100 \times 10^3 \text{ cm}^2/\text{V}\cdot\text{s}$ $n_s \sim 3 \times 10^{15} \text{ m}^{-2}$ CW-ESR light/gate populated	Exp.: $T_2^{B\perp z} = 12 \mu\text{s}$ $T_2^{B\parallel z} = 500 \text{ ns}$ Pred.: $T_2^{B\perp z} = 5 \mu\text{s}$ $T_2^{B\parallel z} = 2.7 \mu\text{s}$	$T_2^{B\parallel z}/T_2^{B\perp z} = 24$ $T_2^{B\parallel z}/T_2^{B\perp z} = 1.9$ $T_1^{B\parallel z}/T_1^{B\perp z} = 0.5$

Table II: Experimental and predicted linewidths and anisotropies for three SiGe heterostructures. Linewidth lifetimes are calculated assuming that the quantum well is completely populated by the donor layer. Accurate analysis is made difficult due to lack of precise values for mobility and density, which are often not measured directly (or reported) for the specific samples addressed with ESR. The magnetic field is assumed to be $B = 0.33$, the standard field in the experimental setups cited.

The DP relaxation also has the counter-intuitive inverse dependence of the spin relaxation time on the momentum relaxation time: $1/T_{1,2} \propto \tau_p$, for small τ_p (or zero field), typical for motional narrowing. We plot the dependence of T_2 on the mobility in Fig. 3. At high mobilities and high frequencies $\omega \gg 1/\tau_p$, we find $1/T_{1,2} \propto 1/\tau_p$.

Discussion We have calculated the transverse and longitudinal relaxation times of a silicon 2DEG in an arbitrary static magnetic field. To test our calculations, we compare them to known ESR data.[1, 2, 19, 22] We limit ourselves to low temperatures, $\epsilon_F \sim 10 - 15$ K, and realistic material parameters for state-of-the-art heterostructures.

The most robust prediction of the theory is the anisotropy, particularly that of T_1 , which is completely independent of all parameters. The only measurement, in Ref. [3], gives satisfactory agreement for T_1 : $T_1^{B\parallel z}/T_1^{B\perp z} = 0.67$ as opposed to the prediction 0.5. Furthermore, the anisotropy of $1/T_2$ goes in the opposite

direction, as it should. The magnitude of this anisotropy is measured to be $T_2^{B\parallel z}/T_2^{B\perp z} = 12.5$. The relaxation times, in the range from about 0.5 to 5 μs , are in rough agreement with what one gets from estimates assuming that this well is a device of type 1.

Table II details results for two other samples as well, also nominally of type 1 for which measurements of T_2 have been performed. Agreement is good for the the sample of Ref.[19], particularly for the anisotropy of T_2 . This is a donor-layer-populated sample, which means that setting the electron density equal to the ion density in the donor-layer is reasonably well-justified. Agreement is considerably less good for the sample in Ref. [1]. Here the mobility is not well-known, and the sample is partially populated by illumination. The position of the ionized centers which populate the well is important for the calculation of the electric field which is thus hard to characterize. Photoelectrons created with light at the bandgap energy may also have symmetry changing effects. This may explain why the Rashba coefficient derived from varying the 2DEG density by light in Ref. [19] appears to be independent of density. Further experimental work along the lines of measuring the density, mobility, T_1 , and T_2 on the same samples is needed.

Other mechanisms may become important as we leave the parameter range considered in this paper. Electron-electron collisions which do not greatly affect the mobility at low temperatures may start to contribute at higher temperatures and mobilities, as they appear to do in GaAs quantum wells.[23] These collisions will also relax the spin, but the relation between momentum relaxation and spin relaxation is not expected to be the same as for the elastic collisions considered here. At higher magnetic fields, the cyclotron motion of the electrons is important. When $\omega_c \tau_p \geq 1$, the average value of the momentum perpendicular to the magnetic field shrinks, reducing or even eliminating DP spin relaxation.[13] This effect may become important at very high mobilities and would be dependent on magnetic field angle. Finally, the addition of details related to the presence of two conduction-band valleys may differentiate further the case of Si from that of GaAs. Golub and Ivchenko [24] have considered spin relaxation in symmetrical ($\alpha=0$) SiGe QWs, where valley domains (even or odd monolayer regions of the QW) may have influence over spin dynamics.

Long spin relaxation times on the order of microseconds, found in presently available SiGe quantum wells, hold great promise for both quantum information processing and spintronics. Our results demonstrate that decreasing the reflection asymmetry within the device will appreciably decrease the Rashba coefficient and the consequent spin relaxation at low temperatures. This can be achieved by a symmetric doping profile or using an external electric field to cancel out the field of the ions. As higher mobility and more exotic SiGe heterostructures are grown and characterized, new physics may emerge.

Acknowledgements

The authors would like to acknowledge useful conversations with Mark Friesen and Jim Truitt and with the rest

of the Wisconsin-Madison solid-state quantum computing group.[26] This work has been supported by the Army Research Office through ARDA and the NSF QUBIC program NSF-ITR-0130400.

[1] W. Jantsch, Z. Wilamowski, N. Sanderfeld, M. Muhlberger, and F. Schaffler, *Physica E* **13**, 504 (2002).

[2] A. M. Tyryshkin, S. A. Lyon, A. V. Astashkin, and A. M. Raitsimring, arxiv/cond-mat 0304284 (2003).

[3] A. M. Tyryshkin, S. A. Lyon, A. V. Astashkin, and A. M. Raitsimring, *Phys. Rev. B* **68**, 193207 (2003).

[4] R. de Sousa and S. D. Sarma, arxiv/cond-mat 0211567 (2003).

[5] L. Roth, *Phys. Rev.* **118**, 1534 (1960).

[6] H. Hasegawa, *Phys. Rev.* **118**, 1523 (1960).

[7] A. V. Khaetskii and Y. V. Nazarov, *Phys. Rev. B* **64**, 125316 (2001).

[8] D. Pines, J. Bardeen, and C. P. Slichter, *Phys. Rev.* **106**, 489 (1957).

[9] E. Abrahams, *Phys. Rev.* **107**, 491 (1957).

[10] D. K. Wilson and G. Feher, *Phys. Rev.* **124**, 1068 (1961).

[11] M. D'yakonov and V. Perel', *Sov. Phys. Solid State* **13**, 3023 (1972).

[12] M. D'yakonov and V. Kachorovskii', *Sov. Phys. Semicond.* **20**, 110 (1986).

[13] B. P. Zakharchenya, *Modern Problems in CM Sciences V.8: Optical Orientation* (North-Holland, 1984).

[14] M. Friesen, P. Rugheimer, D. E. Savage, M. G. Lagally, D. W. van der Weide, R. Joynt, and M. A. Eriksson, *Phys. Rev. B* **67**, 121301 (2003).

[15] M. H. Jones and S. H. Jones, *Virginia Semiconductor* (2002).

[16] H. Jiang and E. Yablonovitch, *Phys. Rev. B* **64**, 041307(R) (2001).

[17] Y. Bychkov and E. Rashba, *J. Phys. C* **17**, 6039 (1984).

[18] E. A. de Andrada e Silva, G. C. L. Rocca, and F. Bassani, *Phys. Rev. B* **55**, 16293 (1997).

[19] Z. Wilamowski, W. Jantsch, H. Malissa, and U. Rossler, *Phys. Rev. B* **66**, 195315 (2002).

[20] C. P. Slichter, *Principles of Magnetic Resonance* (Springer-Verlag, 1978).

[21] A. A. Burkov and A. H. MacDonald, arxiv/cond-mat 0311328 (2003).

[22] Z. Wilamowski and W. Jantsch, *Physica E* **12**, 439 (2002).

[23] M. Glazov, E. Ivchenko, M. Brand, O. Karimov, and R. Harley, arxiv/cond-mat 0305260 (2003).

[24] L. Golub and E. Ivchenko, arxiv/cond-mat 0310200 (2003).

[25] Note that [19] uses the wrong expression for the Fermi wavevector, failing to include the valley degeneracy, so their data analysis is off by a factor of $\sqrt{2}$.

[26] <http://qc.physics.wisc.edu/>